A study of photoelectron recapture due to post-collision interaction in Ne at the 1s photoionization threshold

U Hergenhahn[1,2], A de Fanis[3]†, G Prümper[1], A K Kazansky[4], N M Kabachnik[1,5,6] and K Ueda[1]‡

[1] Institute of Multidisciplinary Research for Advanced Materials, Tohoku University, Sendai 980-8577, Japan

[2] Max-Planck-Institut für Plasmaphysik, EURATOM association, Boltzmannstr. 2, 85748 Garching, Germany

[3] Japan Synchrotron Radiation Research Institute, Sayo-gun, Hyogo 679-5198, Japan

[4] Fock Institute of Physics, State University of Sankt-Petersburg, 198504 Sankt-Petersburg, Russia

[5] Fakultät für Physik, Universität Bielefeld, D-33615 Bielefeld, Germany

[6] Institute of Nuclear Physics, Moscow State University, Moscow 119992, Russia

Abstract. Electron spectra from radiationless decay of Ne 1s vacancy are measured with excitation energies immediately at the 1s ionization threshold. Special attention is given to the excess energy region $|\tilde{E}| < 2\Gamma$ where Γ is the life-time width of the 1s vacancy. Spectra are dominated by recapture of photoelectrons into Rydberg states of Ne^+ above the threshold, and by a smooth transition into the spectator resonant Auger spectrum below the threshold. High resolution of the present experiment allowed us to clearly observe Rydberg states up to $n = 8$ and to determine the individual probabilities of population of these states in the process of photoelectron recapture. Results are compared with calculations based on the semiclassical theory of post-collision interaction extended to high Rydberg excitations of the primary photoexcited electron, as well as with the non-stationary quantum mechanical theory of near-threshold photoionization with the following Auger decay.

12 June 2005

† Present address: Shimadzu Research Laboratory, Wharfside, Trafford Wharf Road, Manchester, M17 1GP United Kingdom

‡ e-mail: ueda@tagen.tohoku.ac.jp

1. Introduction

Inner-shell photoionization of light and medium atoms is usually accompanied by a radiationless (Auger) relaxation process. As a result a photoelectron and an Auger electron are emitted and a doubly charged ion is produced. However, if the photon energy is just above the photoionization threshold the slow photoelectron can still be near the atom when the Auger decay occurs. The Coulomb interaction of the three charged particles in the final state, dubbed the post-collision interaction (PCI), can lead to a recapture of the photoelectron by the doubly charged ion into a high Rydberg state. Thus only the Auger electron is emitted, its energy being different from the diagram value, and an excited singly charged ion is formed. Photoelectron recapture is one part of a broader class of phenomena caused by PCI. It should be considered in the context of the more general problem of a transition from the regime of resonant Auger decay induced by photoexcitation below the threshold to the regime of photoionization followed by Auger decay above the threshold.

The evolution of the photoemission process through an inner-shell ionization threshold has been studied both theoretically and experimentally for a number of cases (Armen *et al* 1985, 1996, 1997, Levin *et al* 1990, Čubrić *et al* 1992, 1993, Ueda *et al* 1996, Aksela *et al* 1997, LeBrun *et al* 1999, Okada *et al* 2005). With a special attention to the photoelectron recapture the near-threshold photoionization was studied by Eberhardt *et al* (1988), Samson *et al* (1996, 1997) and Lu *et al* (1998). Recently, the photoelectron recapture after Ne 1s excitation was observed by detecting the second-step Auger decay (Hentges *et al* 2004, De Fanis *et al* 2004, 2005). A theoretical description of the photoelectron recapture is usually based on a more general consideration of the PCI effects and the resonant Auger transitions. Both the semiclassical approach (Eberhardt *et al* 1988) and quantum theory (Amusia *et al* 1977, Sheinerman 2003) including the resonant scattering theory of Auger processes (Tulkki *et al* 1990, Armen and Levin 1997) were successfully applied to describe the main features of the recapture and more generally the evolution of the photoemission across the threshold from the resonant Auger decay below the threshold to the PCI distorted Auger line above it.

Generally, it is known that only for excitation into the lowest unoccupied nl level, the favoured channel of spectator resonant Auger decay is into a final state with the same nl. For higher excitations, the behaviour changes to shake-modified resonant Auger decay with a transition of the outer electron nl to the $n'l$ orbital where $n' \neq n$. Shakeup into states with $n' > n$ is far more probable than shakedown. This can be understood from the overlap of the respective Rydberg single particle wavefunctions (Ueda *et al* 1996, Armen 1996, Armen *et al* 2000). On the other side, above the threshold the slow photoelectron is 'shaken down' during the Auger decay and even recaptured by the ion. This means that there is a *transition regime* where these two tendencies are blended. According to Whitfield *et al* (1991) and Åberg (1992) the transition regime covers the excess energies between $-\Gamma^{2/3}/2 < \tilde{E} < 2\Gamma$. (The excess energy $\tilde{E}$ is defined as the difference between the photon energy and the ionization potential, $\tilde{E} = \omega - IP$, Γ is

the Auger decay width, and atomic units are used.) In this energy interval the model of shake-modified spectator decay loses its descriptive power, since the intermediate state is composed of several coherently excited Rydberg levels. For the case of the Mg 2p excitations discussed by Whitfield *et al*, the transition regime, however, could not be probed experimentally, since the lifetime broadening of the excited levels is only a few meV. Some measurements of the Auger electron spectra within the transition regime were later made by Aksela *et al* (1997) for Xe $4d_{5/2}$ and Kr $3d_{5/2}$ excitations. They observed a gradual transition from shakeup to shakedown lines and then to the PCI Auger profile without, however, a detailed quantitative analysis. Calculations within the transition regime were carried out by Armen *et al* (1996, 1997). They used the quantum mechanical resonant scattering theory approach to Auger decay originally developed by Åberg and Howat (1982), and included the interference between different intermediate states. The calculations agreed well with the experiment which was done, however, with rather poor resolution. In spite of these investigations, a detailed knowledge of the photoelectron recapture especially in the transition regime is still missing and its further investigation is desirable.

In the present paper we report the results of high resolution measurements of the radiationless decay of a Ne 1s vacancy into states with a $2p^4\,(^1D_2)$ ion core. Our measurements cover the energy range from 0.5 eV below to 3.6 eV above the 1s ionization potential. Within this region, the decay spectrum develops from resonant Auger transitions to the Ne^+ $2p^4\,(^1D_2)np$ states into a part of the normal Ne K-$L_{2,3}L_{2,3}$ Auger spectrum. Since the lifetime broadening of the Ne 1s vacancy state is 270 meV (Coreno *et al* 1999), the transition regime discussed above reaches from approximately −630 meV to 540 meV, and is nearly completely covered by our measurements. High resolution of our experiment allowed to resolve the ionic Rydberg states up to $n = 8$ and to investigate the probability of photoelectron recapture to individual Rydberg states as a function of the excess energy for the first time.

The process we consider is

$$\mathrm{Ne} + \mathrm{h}\nu \rightarrow \mathrm{Ne}\ 1s^{-1}(n,\varepsilon)p \rightarrow \mathrm{Ne}\ 2p^4(^1D_2)(n',\varepsilon')p + e^-_A. \qquad (1)$$

The notation (n, ε) indicates a photo- or Rydberg electron. Dependent on the values of n or ε and its primed counterparts, the reaction equation (1) describes resonant Auger decay, shake-off, photoelectron recapture or sequential photo-double ionization. In the case of photoelectron recapture in the final state, the singly charged ion with a configuration Ne $2p^4(^1D_2)n'p$ is energetically located above the double ionization potential of Ne for $n' \geq 5$. By that, these states will autoionize to the $2p^4(^3P)$ manifold by emission of a low kinetic energy Auger electron (valence intermultiplet Auger transition). These second-step Auger electrons, with kinetic energies below 3.1 eV, were recently observed by some of the authors (De Fanis *et al* 2004, 2005) and for other intermediate states by Hentges *et al* (2004). Due to their low energy, they allow to characterize the energy positions of the Ne^+ $n'p$ Rydberg series with unprecedented detail. In this article we report on the electrons emitted in the first step

of the Auger cascade (e_A^- in (1)). These have kinetic energies on the order of 806 eV. Since both processes probe properties of the intermediate ionic Rydberg states, these studies are complementary.

We compare our experimental results with two types of calculations. One is based on a semiclassical approach and is an extension of the model by Russek and Mehlhorn (1986). Another is based on the quantum mechanical non-stationary theory of near-threshold photoionization recently developed by two of the authors (Kazansky and Kabachnik 2005). Atomic units are used throughout unless otherwise indicated.

2. Experiment

The measurements have been performed at the c-branch of the beamline 27SU at the SPring-8 synchrotron radiation source in Japan. This beamline is equipped with a so-called figure-8 undulator (Tanaka *et al* 1999), which is capable of producing linearly polarized light with the electric field vector in the storage ring plane or perpendicular to it. In the c-branch, the photons from this insertion device are monochromatized by a Hettrick-type varied line space plane grating monochromator (Ohashi *et al* 2001). For the measurements reported here, grating 1 was used, with the photon resolution set to about 95 meV. The target consists of a gas cell equipped with electrodes to provide small static electric fields along the beam direction, and electrons are detected by a hemispherical electrostatic analyzer (Gammadata-Scienta SES2002) mounted horizontally and perpendicular to the photon beam. All spectra reported here were recorded with horizontal polarization. The pass energy was set to 100 eV, giving an analyzer resolution of about 66 meV.

The kinetic energy scale before the start of the measurements was calibrated to the energy of the resonant Auger decay to the $2p^4(^1D_2)3p(^2P)$ state recorded on the maximum of the 1s-3p resonance. Using a final state energy of 55.835 eV (Bolognesi *et al* 2002) and a resonance energy of 867.12(5) eV (Coreno *et al* 1999), this decay appears at 811.29 eV kinetic energy. Ion yield scans were used to locate the 1s-np resonances of Ne and to calibrate the photon energy scale using the reference energy given above. The spectra were then converted to a binding energy scale. This nevertheless resulted in final state energies of the $2p^4n$p states which were systematically larger than the zero kinetic energy results of Bolognesi *et al*, on average by 70 meV, and which fluctuated by about 80 meV between different spectra. For the determination of escape probabilities, therefore the position of the double ionization potential (DIP), 65.72 eV (Bolognesi *et al* 2002), was located relative to the observed positions of the Ne $2p^4n$p, $n = 4 - 8$ final states.

The central quantity in our article is the excess energy, that is the photon energy relative to the Ne 1s ionization potential (IP). The latter value could not be determined directly in this article, but had to be taken from the literature. Reported values do not completely agree, dependent on the technique by which they have been determined (Hitchcock and Brion 1980, Sæthre *et al* 1984, Coreno *et al* 1999). We have adopted the

value of 870.17(5) eV cited by Coreno *et al* (1999). Since we have used the energy of the 1s-3p resonance to calibrate our photon energy scale, the accuracy of the Ne 1s IP relative to the energy of the resonance is more important than its absolute value. In a very recent experiment, the Ne 1s-np Rydberg series was remeasured by photoabsorption, and the series limit was found at 870.15(4) meV using the same normalization for the 1s-3p resonance (Kato *et al* 2005). In summary we assume an experimental inaccuracy of our excess energies of 85 meV, plus a scale error of 85 meV common to all data points.

To extract the recapture probabilities into the Ne $2p^4(^1D_2)np$ states with $n = 3-6$, the total area of the respective line, reduced by a linear background, was determined and then divided by the total area of all structure pertaining to the transition (1). Beforehand the measured spectra were divided by a factor to account for the fact that one electron illuminates several pixels of the CCD camera, which reads out the SES2002 electron detector ('Multiple Counting Factor'). The resulting areas are approximately Poissonian, and error bars quoted have been calculated on this basis. For $n = 7, 8$ areas were extracted by fitting Gaussian curves to these structures.

3. Theory

As discussed in the Introduction, a very slow photoelectron can be recaptured by the ion due to PCI, namely due to an increase of the effective Coulomb attraction between the core and the photoelectron after Auger decay. This process corresponds to the high kinetic energy tail of the Auger electron distribution. Since the photoelectron recapture has to lead into discrete final states, the continuous PCI distorted Auger electron distribution changes into a series of spectator resonant Auger lines. We intend to describe the intensity distribution of the continuum and the discrete part of Auger emission by theoretical models. We will first recall the main features of a semiclassical model for PCI, of which we have carried out a numerical implementation. In the following subsection we will describe the application of a new model for Auger decay in the vicinity of an inner-shell threshold, which is based on a time-dependent quantum mechanical theory (Kazansky and Kabachnik 2005). This *ansatz* is free from the restrictions and shortcomings of stationary PCI models, which have been cited above.

3.1. Semiclassical theory

In existing semiclassical theories for PCI, the distorted profiles of photoelectron or Auger lines have usually been derived with excess energies $\tilde{E} \gg \Gamma$ in mind. It is therefore not *a priori* granted that they are applicable in the range of $\tilde{E} \sim \Gamma$, and to cases where eventually no photoelectron is emitted. Below we reanalyze the derivation of one group of semiclassical models of PCI, summarized by Russek and Mehlhorn (1986), and generalize it to the case of resonant Auger emission. We carry out numerical calculations of Auger and resonant Auger profiles with this model. In this article we

call it the Russek-Mehlhorn (RM) model of PCI, although a number of other authors deserve credits for it, which are named in the reference given above. It can be intuitively derived by considering the energy dependent Auger line shape as a Fourier transform of the exponential decay curve of the excited state

$$a(E) = \left(\frac{\Gamma}{2\pi}\right)^{1/2} \int_0^\infty dt\, \exp\Big[-\int_0^t dt' \left(\frac{\Gamma}{2} + iE\right)\Big] , \tag{2}$$

where $a(E)$ is the Auger amplitude, E the Auger energy, expressed as a difference to the nominal Auger energy E_A. The nominal Auger energy is observed in the case of no PCI, that is for $\tilde{E} \gg E_A$.

Equation (2) is manipulated by introducing the energy change of the Auger electrons, asymptotically detected with energy E, due to the interaction with the photoelectron. Naming this quantity S_A one has

$$a(E) = \left(\frac{\Gamma}{2\pi}\right)^{1/2} \int_0^\infty dt\, \exp\Big[-\int_0^t dt' \left(\Gamma/2 + i(E - S_A(E_A, \tilde{E}, t'))\right) \Big] . \tag{3}$$

The crucial point is the determination of the unknown function $S_A(E_A, \tilde{E}, t')$. For this, Russek and Mehlhorn represented the photoelectron by an outgoing spherical wave (s-wave), the same for the Auger electron, which starts with some time delay t. Then, at the radius ρ where the Auger electron overtakes the photoelectron, the former gains the amount of energy ρ^{-1} due to the change in screening of the nuclear core by one unit. For a calculation of ρ, the time elapsed for travel of the respective electron from its initial radius in the atom to the distance ρ is expressed as an integral of $1/v$ over r (v, a momentary velocity and r, a position of the electron), and the respective integrals for photo- and Auger electron are required to be equal:

$$\int_{R_s}^{\rho} dr\, \frac{1}{(2(\tilde{E} + 1/r))^{1/2}} = \int_{R_A}^{\rho} dr\, \frac{1}{(2(E_A + 2/r))^{1/2}} + t\ . \tag{4}$$

Here, R_s and R_A are the initial radii of photoelectron and Auger electron. The denominator of the integrand contains the momentary Coulomb energy of the electron Z/r. The small difference of the actual Auger electron energy to the nominal Auger energy E_A has been neglected.

Up to this point, this formulation of the problem does not rely on restrictive assumptions for the energies of the two electrons involved, apart from $\tilde{E} < E_A$. Intuitively it is clear that a solution of equation (4) exists for very small and even negative $\tilde{E}$. Due to the simplicity and the classical *ansatz* of the model, the discretization of Auger energies in the case of photoelectron recapture or negative excess energies is not reproduced. We can, however, hope that the continuous energy distribution produced by this model mimics the distribution of intensities of the resonant Auger lines.

We proceeded by analytically solving the integrals in equation (4). This gives an implicit solution of the upper integration boundary ρ, and thus the energy exchange $\rho^{-1} = S_A$ for each value of $E_A, \tilde{E}$ and time delay of the Auger electron t. Using this we have calculated the Auger lineshape as the square of the complex amplitude given in equation (3). Details can be found in the appendix.

Here, one caveat should be noted: the PCI theory discussed in this article describes the interaction of one photoelectron with one Auger electron. The $2p^4\,(^1D_2)np$ states discussed in this article, however, decay by emission of another low kinetic energy electron into the $2p^4\,(^3P)$ manifold (De Fanis *et al* 2004, 2005). We have not attempted to take into account their influence on the primary Auger decays.

3.2. Quantum theory

Existing quantum mechanical approaches to the problem of photoelectron recapture due to PCI in photoionization are based on a stationary formalism. In this paper we use an alternative time-dependent quantum-mechanical approach, which allows us to avoid difficulties inherent in some stationary formulations (*e.g.* Armen and Levin 1997), such as summation over infinite number of intermediate states and interference of the intermediate states in the transition regime. A version of the non-stationary theory of near-threshold photoionization of inner atomic shells was recently developed by two of the authors and will be published in detail elsewhere (Kazansky and Kabachnik 2005). Here we only give a short description of the approach.

We consider the problem of interaction of a weak electromagnetic field with an atom in the vicinity of an isolated inner-shell ionization threshold. In this case the solution of the non-stationary Schrödinger equation for the total wavefunction of the system can be reduced to the solution of a system of integro-differential equations for basis functions describing the state of the excited (Rydberg) electron in the Ne ion with 1s hole, $\phi_d(\vec{r},t)$, and the state of this electron, $\phi_\epsilon(\vec{r},t)$, after the Auger decay with Ne remaining in the $2p^{-2}$ state and with the Auger electron emitted with energy ϵ (so called Fano-Feshbach problem):

$$i\frac{\partial\phi_d(\vec{r},t)}{\partial t} = \hat{H}_1(\vec{r})\phi_d(\vec{r},t) - \vec{d}\cdot\vec{\mathcal{E}}(t)\phi_0(\vec{r})\exp(-i\epsilon_0 t) + \int d\epsilon\, V_\epsilon\phi_\epsilon(\vec{r},t)\;, \tag{5}$$

$$i\frac{\partial\phi_\epsilon(\vec{r},t)}{\partial t} = (\hat{H}_2(\vec{r}) + \epsilon)\phi_\epsilon(\vec{r},t) + V_\epsilon^*\phi_d(\vec{r},t)\;. \tag{6}$$

Here $\phi_0(\vec{r})$ is the initial state of the active electron in the ground state of the atom with the energy ϵ_0, $\vec{d}$ is a dipole operator, $\vec{\mathcal{E}}(t)$ is the electric field of the electromagnetic pulse, V_ϵ is the interaction between the discrete state $\phi_d(\vec{r},t)$ and the continuum $\phi_\epsilon(\vec{r},t)$ which is responsible for the decay. The single-electron Hamiltonians $\hat{H}_1(\vec{r})$ and $\hat{H}_2(\vec{r})$ describe the motion of the electron before and after the decay. Note that asymptotically the potential in the Hamiltonian $H_1(\vec{r})$ behaves as $1/r$, since it results from a singly charged ion with a vacancy in an inner shell. The Hamiltonian $H_2(\vec{r})$ contains the potential of the doubly charged ion with asymptotic behavior $2/r$. It is supposed that the Auger electron is fast and its interaction with the Rydberg electron is ignored.

Since ϵ is a continuum energy, the above equations in fact constitute a system of the infinite number of coupled equations and its solution is a formidable task. The simplest way to decouple the infinite number of equations describing the continuum

spectrum is to assume that the interaction V_ϵ is independent of energy. This corresponds to Fano's approach to autoionization resonances (Fano 1961). In the time-dependent formulation of theory this leads to the introduction of an effective complex Hamiltonian $\hat{H}_1 - i\Gamma/2$, the imaginary part of which describes the attenuation of the state due to the Auger decay. In this way the above system can be reduced to a single non-homogenous differential equation:

$$i\frac{\partial\phi_d(\vec{r},t)}{\partial t} = \left(\hat{H}_1(\vec{r}) - i\frac{\Gamma}{2}\right)\phi_d(\vec{r},t) - \vec{d}\cdot\vec{\mathcal{E}}(t)\phi_0(\vec{r})\exp(-i\epsilon_0 t)\ , \tag{7}$$

where $\Gamma = 2\pi|V|^2$. Formally similar equations have been derived and considered for the Auger decay of dissociating molecules (Pahl *et al* 1996, Gortel *et al* 1998).

A solution of equation (7) describes the development of the wave packet which is pumped by the pulse $\vec{\mathcal{E}}(t)$ and at the same time is subject to the Auger decay with the rate $1/\Gamma$. However, the intermediate state $|\phi_d(\vec{r},t)\rangle$ is not physically observable since it disappears at asymptotically large t. Only the final states $|\phi_\epsilon(\vec{r},t)\rangle$ have physical meaning: they describe the state of the Rydberg electron when the Auger electron is emitted with the energy ϵ. One can show, however, that if the Auger electron is not observed then the probability of populating any Rydberg state of the final ion $|\psi_n(\vec{r})\rangle$ can be calculated as a squared projection of this state onto the wave packet of the intermediate state at the moment t, integrated over time:

$$P_n = \Gamma\int dt\,|\langle\psi_n(\vec{r})|\phi_d(\vec{r},t)\rangle|^2\ . \tag{8}$$

The rigorous derivation of this equation will be given elsewhere (Kazansky and Kabachnik 2005). Similarly, one can show that the probability to find the excited (Rydberg) electron in the continuum with a certain energy E is given by

$$P_E = \Gamma\int dt\,|\langle\psi_E(\vec{r})|\phi_d(\vec{r},t)\rangle|^2\ , \tag{9}$$

where $\psi_E(\vec{r})$ is a continuum wave function of the Rydberg electron:

$$(\hat{H}_2(\vec{r}) - E)\psi_E(\vec{r}) = 0\ . \tag{10}$$

In numerical calculations presented below we have used the Hartree-Slater approximation for calculating the local potentials in Hamiltonian $H_1(\vec{r})$ for a Ne ion with a 1s vacancy before the Auger decay and in $H_2(\vec{r})$ with two 2p vacancies for the final state after the Auger decay. Equation (7) has been numerically solved on a non-uniform grid by application of the Crank–Nickolson algorithm. In more details the method of the calculation is described by Kazansky and Kabachnik (2005).

4. Results

In this section, we will first discuss some representative electron spectra. Then, we derive values of the recapture probability from a series of spectra we have measured, and finally discuss the state-dependent recapture probability.

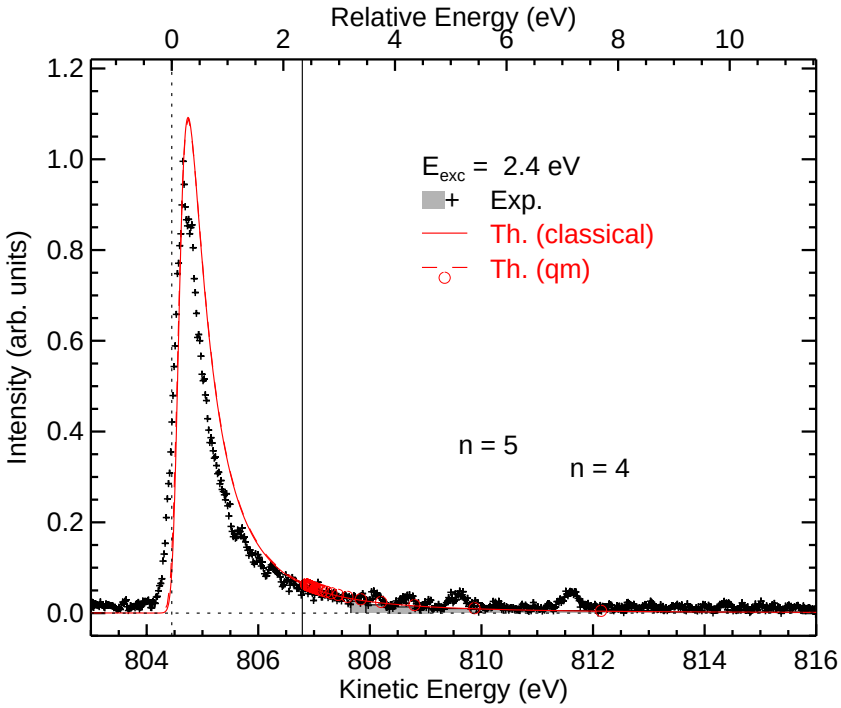

Figure 1. Part of the Ne KLL Auger and resonant Auger spectrum at an excitation energy of 2.4 eV above the 1s ionization threshold. The spectrum shows the KLL Auger decay to the Ne^{2+} $2p^4$ ($^1D_2$) state at lower kinetic energies and decays into Ne^+ $2p^4(^1D_2)np$ singly ionized states at higher kinetic energies, where the np Rydberg levels are populated by recapture of the photoelectron. +: Experimental data points after subtraction of a constant background; solid and dashed lines: theoretical Auger electron profiles calculated using the semiclassical RM model and the non-stationary quantum- mechanical model, respectively. Intensities for recapture into discrete states calculated by the quantum-mechanical model are shown by open circles. Areas of the gray shaded boxes represent the experimental intensity of recapture into the $n = 3 - 8$ states. Normalization of the box widths and of the discrete values calculated by the quantum mechanical theory is chosen appropriately for a continuation of the Auger part of the spectrum (Fano and Cooper 1968). To ease comparison the experimental spectra were shifted by the observed deviation to the literature final state energy, see experimental section. The vertical dotted line shows the nominal Auger energy E_A, the vertical solid line shows the difference between photon energy and Ne^{2+} double ionization potential. The part of the spectrum on the high kinetic energy side of this line pertains to recapture processes.

4.1. Electron spectra

Typical results of our measurements and calculations are shown in figure 1. Excited 2.4 eV above the 1s threshold, this spectrum still shows clearly visible spectral features for recapture of the photoelectron into $n = 4 - 7$ Rydberg states. For recapture into orbitals with lower binding energies the signal becomes a smooth continuation of the Auger spectrum at this apparatus resolution. The spectrum have a typical shape of the PCI distorted Auger line and a shift upwards in energy with respect

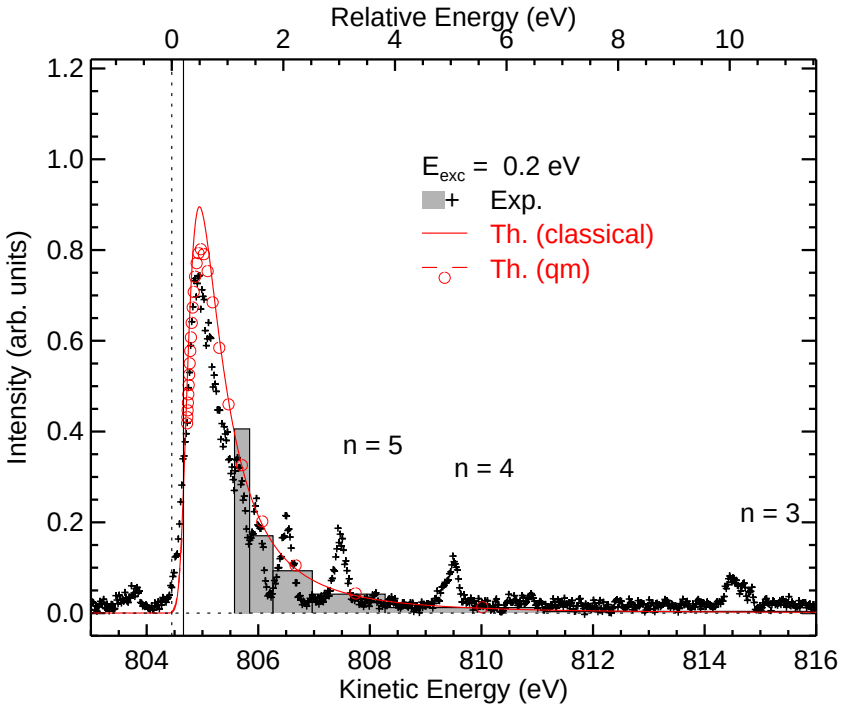

Figure 2. Ne K-shell radiationless decay spectrum into $Ne^{2+}\,2p^4\,(^1D_2)$ and $Ne^{+}\,2p^4(^1D_2)np$ final states, excited at $\tilde{E} = 0.2$ eV, i.e. at excitation energy 0.2 eV above the 1s ionization threshold. Notations are the same as in figure 1.

to its diagram position as is well known from many previous studies of the PCI effects (Schmidt 1997). The solid line shows the result of the semiclassical RM calculation which have been convoluted with a Gaussian width of 116 meV to account for experimental broadening. The dashed line which almost coincides with the solid one, represents the result of the corresponding non-stationary quantum-mechanical calculation. Experimental and theoretical profiles are normalized to equal area. Both calculations, semiclassical and quantum-mechanical, give practically identical results. A comparison of the experimental spectrum with our calculated profiles shows a good agreement of the general shape. Both curves are slightly shifted to higher energies with respect to experimental points. This shift, which is seen also in all other spectra, can probably be explained by inaccuracy of experimental energy calibration which is about 120 meV. The general intensity distribution in the recapture part of the spectrum is well reproduced by both the extended PCI profile from the RM calculation and by probabilities calculated quantum-mechanically, which can best be seen when they are compared with a continuous representation of the *experimental* line strength represented by the gray shaded boxes (Fano and Cooper 1968, Tulkki *et al* 1990). To determine the position of the boxes which give the experimental intensities in figures 1-4 we used the value of quantum defect of the series which was obtained in experiment by De Fanis *et al* (2005).

When approaching the threshold, more and more intensity is found at energies below

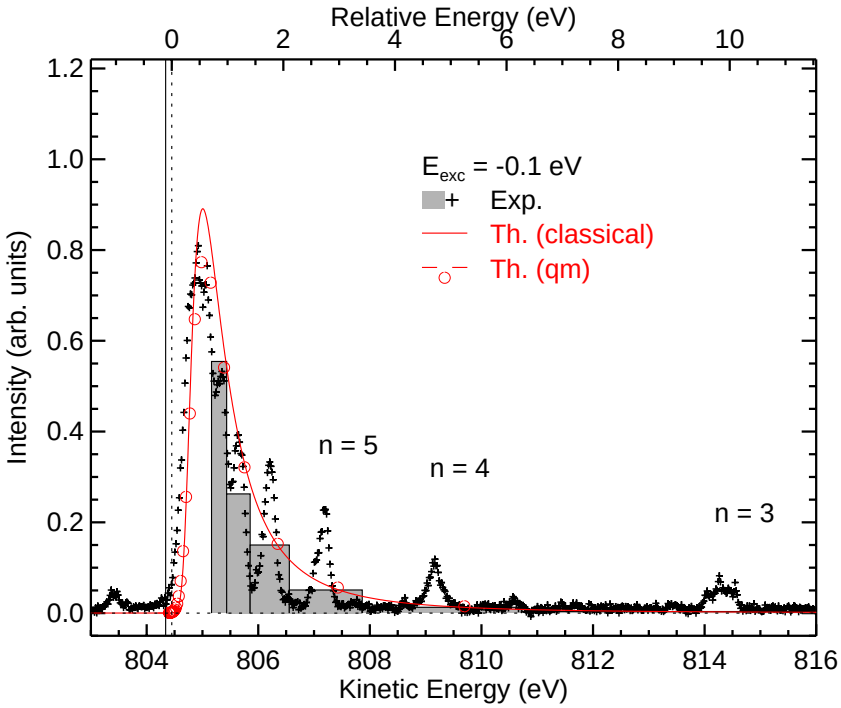

Figure 3. Ne K-shell radiationless decay spectrum into $Ne^{2+}\,2p^4\,(^1D_2)$ and $Ne^{+}\,2p^4(^1D_2)np$ final states, excited at $\tilde{E} = -0.1$ eV, i.e. at excitation energy 0.1 eV below the 1s ionization threshold. Notations are the same as in figure 1.

the respective $Ne^{2+}\,2p^4(^1D_2)$ double ionization threshold, which leads to singly ionized states. At the photon energy 0.2 eV above the 1s threshold only a small fraction of the 1s excited electrons is actually ionized into the continuum (figure 2). The maximum of the spectrum is already in the region which corresponds to Rydberg excitations. Both calculations reproduce well the experimental intensity distribution of the resolved resonant Auger lines as well as the shape of the spectrum in the region of the unresolved Rydberg states and continuum states close to the double ionization threshold.

The radiationless decay spectrum at a photon energy -0.1 eV below the Ne 1s IP (figure 3) would properly be termed spectator resonant Auger spectrum. The envelope of the resonant Auger spectrum is well reproduced by the RM model extended to primary electron energies pertaining to Rydberg excitations as well as by our rigorous quantum-mechanical calculation. This excitation energy approximately corresponds to the Ne 1s $\rightarrow$ 12p excitation. The most intensive from the resolved lines is $n = 8$. Therefore, it is plausible to assume that in this case shake-down of the spectator electron is more probable than shake-up. This is confirmed by our theoretical calculations and is in agreement with the speculations of Whitfield *et al* (1991) on a transition from resonant to normal Auger decay. Higher resolution measurements are, however, necessary in order to prove the above statement experimentally.

Finally, in figure 4 we show the spectrum taken at $\tilde{E} = -0.3$ eV, which is already close to the usual resonant Auger spectrum. This excitation energy corresponds to n

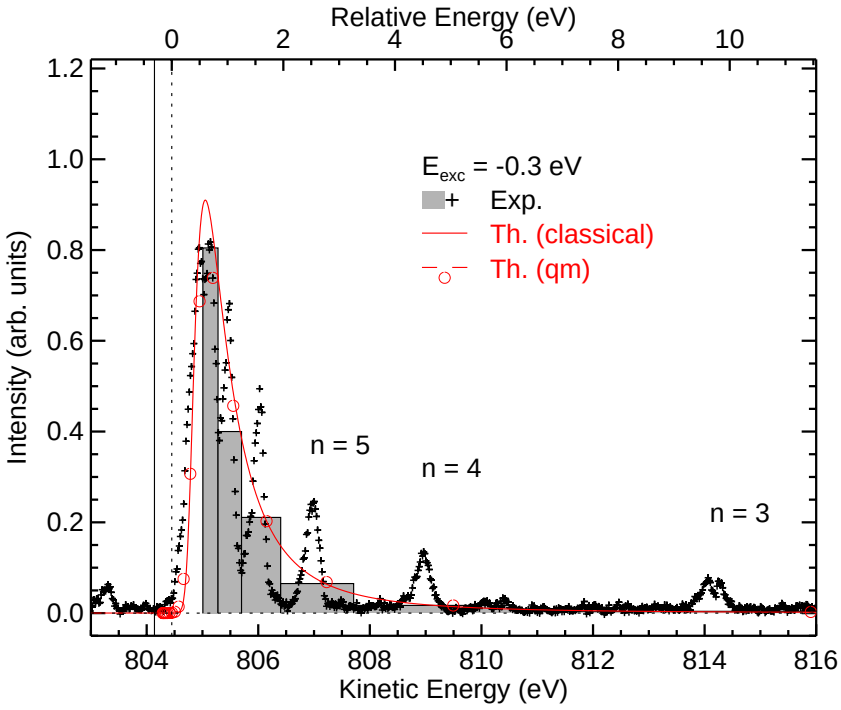

Figure 4. Ne K-shell radiationless decay spectrum into $Ne^{2+}\,2p^4\,(^1D_2)$ and $Ne^{+}\,2p^4(^1D_2)np$ final states, excited at $\tilde{E} = -0.3$ eV, i.e. at excitation energy 0.3 eV below the 1s ionization threshold. Notations are the same as in figure 1.

about 7. The $n = 8$ resonance has maximal intensity showing the shake-up feature of the spectrum. The population of the Rydberg states (and intensity of corresponding resonant Auger transitions) are well reproduced by our calculations. Both theories accurately describe the envelope of the spectrum.

4.2. Recapture probabilities

From the full set of measurements, of which figures 1-4 showed examples, we have derived the energy dependent escape probability as the fraction of experimental intensity at kinetic energies lower than the difference between photon energy and double ionization potential to the $2p^4\,(^1D_2)$ state (figure 5). Even at the highest excess energy which we have measured, 3.6 eV above the threshold, the experimental recapture probability is about 10 %. The intensity of the $2p^4\,(^1D_2)3p$ state is counted as recapture, although some of it might result from 2p shake-up satellites. A quick estimate of the respective cross sections, however, shows that this mechanism should produce an intensity which is 1 % or less than the radiationless transitions to the $2p^4\,(^1D_2)$ ion core. This may still explain most of the deviation to the calculated values at high energies. With respect to the comparison at lower energies, we observe that the onset of 1s photoelectron intensity occurs at kinetic energies of about 0.5 eV, and is found at somewhat lower excess energies in the experimental data. Agreement of the theoretical data with each other is very satisfactory.

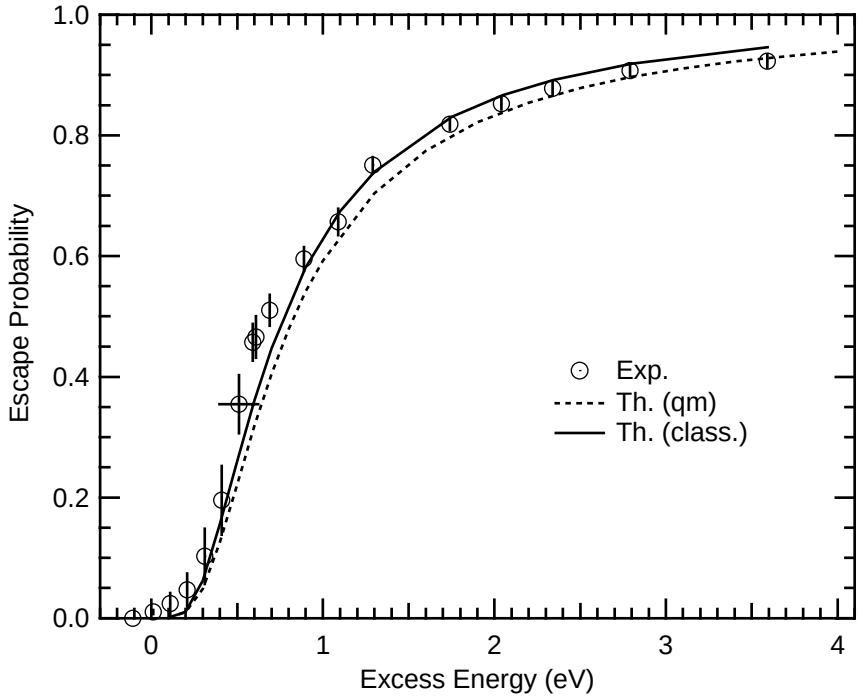

Figure 5. Escape probability for Ne 1s photoelectrons from ions decaying into the $2p^4\,(^1D_2)$ state. Experimental data (open circles) are compared to calculated data. The solid line is calculated using the semiclassical RM model by integrating the negative energy region underneath an Auger electron profile, the dashed line is calculated within the non-stationary quantum-mechanical model. The horizontal error bar is constant for all experimental data.

4.3. State dependent recapture probabilities

The state dependent recapture probabilities as functions of the excess energy are plotted in figure 6. Their dependence on energy is similar apart from the lowest n states. The experimental values are compared with the results of the two calculations. In the semiclassical RM model (solid line) the results are obtained by integrating the respective energy region underneath an Auger electron profile. Dashed line shows the probabilities of recapture to the np Rydberg orbital calculated within the non-stationary quantum-mechanical model using equation (8). One can see from the figure that also for the individual recapture probabilities the two theories give very similar predictions, and the agreement with the experimental data is quite reasonable.

5. Discussion

The term 'post-collision interaction' designates several phenomena due to Coulomb interaction of two charged particles emitted from the same system and the residual ion. It is often implicitly understood that it is a necessary condition for this type of interaction that the interacting partners are in the continuum. Here we have shown that

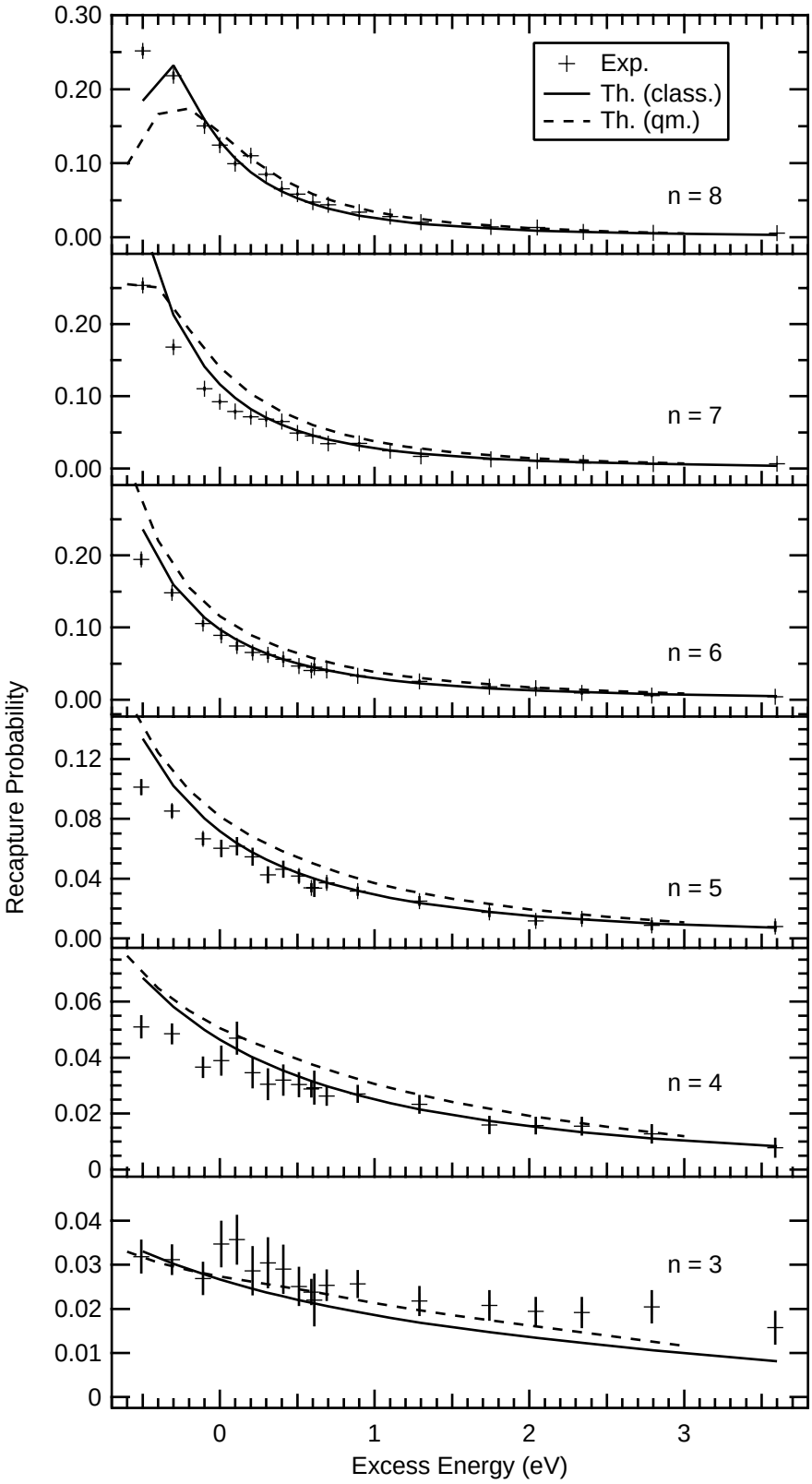

Figure 6. Probability for Ne 1s photoelectrons to be recaptured into an np Rydberg orbital when the ion core undergoes KLL Auger decay into the $2p^4(^1D_2)$ state. Experimental values (+) are compared to data calculated within two models: solid line - semiclassical RM model, dashed line: - non-stationary quantum-mechanical model.

the Coulomb interaction, as taken into account by PCI theory, is also the main factor governing the intensity distribution of recapture into highly excited Rydberg states, and for shake-modified resonant Auger decay of highly excited Rydberg states. We have explicitly probed the energy range between $-(1/2)\Gamma^{2/3} < \tilde{E} < 2\Gamma$, in which earlier investigations expected a change from the predominance of shake-up transitions to a dominance of recapture transitions, which were seen as a type of shake-down transitions (Whitfield *et al* 1991). We would like to note that it is a matter of interpretation whether one sees this behavior of the radiationless decay patterns as a 'transition' between two different regimes. Although the term 'shake-up' suggests an energy gain of the electron, which transits to a higher n, to the contrary these transitions occur because the Rydberg electron does *not* experience a change in energy. In fact, for all but the lowest n the position of the center of gravity of the radiationless decay spectrum decreases linearly in kinetic energy for $\tilde{E} < -(1/2)\Gamma^{2/3}$ and approaches the constant nominal Auger energy for $\tilde{E} > 2\Gamma$.

Comparing figures 1-4 one can follow the gradual transition from the above the threshold region where the PCI-distorted Auger profiles are expected, to the below-threshold region with a typical resonant Auger spectrum. Although the character of the spectrum changes from predominantly continuous to predominantly discrete, the overall intensity distribution, presented by the envelope, changes only slightly and gradually and shows no drastic changes when the photon energy is tuned across the threshold. This observation, made in a high resolution experiment, confirms the data of earlier low-resolution measurements and theoretical expectations.

6. Conclusions

In conclusion, we have measured the Auger electron spectra in near-threshold photoionization of Ne 1s shell. The photon energy was tuned with fine steps across the threshold covering the transition energy region $|\tilde{E}| < 2\Gamma$. High resolution allowed us to determine the population of the Rydberg states with $n = 3 - 8$ due to resonance excitation below and photoelectron recapture above the 1s threshold. We have found that while the character of the spectra is gradually changed from the PCI distorted Auger line profile above the threshold to Rydberg series of the resonant transition below it, the overall intensity distribution does not change much and does not reveal any drastic change when the photon energy passes through the threshold. The experimental data are compared with the calculations based on two different theoretical approaches: semiclassical and time-dependent quantum mechanical. Both approaches give surprisingly similar results. This demonstrates that the semiclassical approach is a robust method of description of the near-threshold phenomena. Both theories agree with the experimental data.

Acknowledgments

This experiment was carried out with the approval of the SPring-8 program advisory committee and supported in part by Grants-in-Aid for Scientific Research from the Japan Society for the Promotion of Science (JSPS). UH and NMK acknowledge the hospitality and financial support of the IMRAM in Tohoku University during their visits. NMK acknowledges the financial support and hospitality of the University of Bielefeld.

Appendix

Equation (4) contains integrals of the type

$$I(E,Z,r) = \int dr\,(2(E+Z/r))^{-1/2} \tag{A.1}$$

which has analytical solutions as for positive so for negative values of E. By the transformation $u = 1/r$ the integral becomes of the form listed in standard tables of integrals. For positive E the solution of Russek and Mehlhorn (1986) was used:

$$I_+(E,Z,u) = \frac{(E+Zu)^{1/2}}{2^{1/2}\,Eu} + \frac{Z}{(2E)^{3/2}}\,\ln\left[\frac{(1+Zu/E)^{1/2}-1}{(1+Zu/E)^{1/2}+1}\right] \qquad (E>0). \tag{A.2}$$

For negative values of E the solution can be presented as

$$I_-(E,Z,u) = \frac{(E+Zu)^{1/2}}{2^{1/2}\,Eu} + \frac{Z}{E(-2E)^{1/2}}\,\mathrm{arctg}\left[\frac{(E+Zu)^{1/2}}{(-E)^{1/2}}\right] \qquad (E<0). \tag{A.3}$$

Using these expressions for the integrals in (4) and inserting the lower limits $1/R_s$, $1/R_A$ and upper limit $S_A = 1/\rho$ we can present equation (4) in the following form:

$$I_\pm(\tilde{E},1,S_A) - I_\pm(\tilde{E},1,1/R_s) - I_+(E_A,2,S_A) + I_+(E_A,2,1/R_A) = t. \tag{A.4}$$

which provides an implicit solution for the upper integration limit $\rho = 1/S_A$ in (4). On the left side of equation (A.4) I_+ (equation (A.2)) or I_- (equation (A.3)) should be used for positive or negative energies of photoelectrons, respectively. Values for the lower integration limits of $R_s = 0.128$ a.u. and $R_A = 0.804$ a.u., found as $\langle r\rangle$ of the 1s and the 2p shells of neutral Ne in a Hartree-Fock calculation (Cowan 1981), were inserted. Further in the calculation, S_A is needed as a function of delay time t between electron and Auger electron emission. The other two variables are fixed, E_A on physical grounds, $\tilde{E}$ because the experimental profiles we compare with what have been recorded at fixed photon energy.

We have therefore calculated the left hand side of (A.4) on a logarithmic grid in r-space. The remaining double integral in (3) was solved by numerical integration on a fine grid of t' values. For each t', the pertaining value of S_A was found by interpolation of the relation between r and t in (A.4). A lifetime of $\Gamma = 268.7$ meV was used in the simulations.

References

Åberg T and Howat G 1982 in *Corpuscles and Radiation in Matter I*, Encyclopedia of Physics Vol. XXXI, ed W Mehlhorn (Berlin:Springer-Verlag) p 469

Åberg T 1992 *Physica Scripta* **T41** 71

Aksela H, Kivilompolo M, Nõmmiste E and Aksela S 1997 *Phys. Rev. Lett.* **79** 4970

Amusia M Ya, Kuchiev M Yu, Sheinerman S A and Sheftel S I 1977 *J. Phys. B: At. Mol. Phys.* **14** L535

Armen G B, Åberg T, Levin J C, Crasemann B, Chen M H, Ice G E and Brown G S 1985 *Phys. Rev. Lett.* **54** 1142

Armen G B 1996 *J. Phys. B: At. Mol. Opt. Phys.* **29** 677

Armen G B, Levin J C and Sellin I A 1996 *Phys. Rev.* A **53** 772

Armen G B, Southworth S H, Levin J C, Arp U, LeBrun T and MacDonald M A 1997 *Phys. Rev.* A **56** R1079

Armen G B and Levin J C 1997 *Phys. Rev.* A **56** 3734

Armen G B, Aksela H, Åberg T and Aksela S 2000 *J. Phys. B: At. Mol. Opt. Phys.* **33** R49

Bolognesi P, Avaldi L, Cooper D R, Coreno M, Camilloni R and King G C 2002 *J. Phys. B: At. Mol. Opt. Phys.* **35** 2927

Coreno M, Avaldi L, Camilloni R, Prince K C, de Simone M, Karvonen J, Colle R and Simonucci S 1999 *Phys. Rev.* A **59** 2494

Cowan R D 1981 *The Theory of Atomic Structure and Spectra* (Berkeley: University of California Press)

Čubrić, Wills A A, Comer J and MacDonald M A 1992 *J. Phys. B: At. Mol. Opt. Phys.* **25** 5069

Čubrić D, Wills A A, Sokell E, Comer J and MacDonald M A 1993 *J. Phys. B: At. Mol. Opt. Phys.* **26** 4425

De Fanis A, Prümper G, Hergenhahn U, Oura M, Kitajima M, Tanaka T, Tanaka H, Fritzsche S, Kabachnik N M and Ueda K 2004 *Phys. Rev.* A **70** 040702

De Fanis A, Prümper G, Hergenhahn U, Kukk E, Tanaka T, Kitajima M, Tanaka H, Oura M, Fritzsche S, Kabachnik N M and Ueda K 2005 *J. Phys. B: At. Mol. Opt. Phys.* accepted

Eberhardt W, Bernstorff S, Jochims H W, Whitfield S B and Crasemann B 1988 *Phys. Rev.* A **38** 3808

Fano U 1961 *Phys. Rev.* **124** 1866

Fano U and Cooper J W 1968 *Rev. Mod. Phys.* **40** 441

Gortel Z W, Teshima R and Menzel D 1998 *Phys. Rev.* A **58** 1225

Kato M, Morishita Y, Koike F, Oura M, Yamaoka H, Tamenori Y, Okada K, Matsudo T, Gejo T, Suzuki I H and Saito N 2005 to be submitted to *Phys. Rev.* A

Hentges R, Müller N, Viefhaus J, Heinzmann U and Becker U 2004 *J. Phys. B: At. Mol. Opt. Phys.* **37** L267

Hitchcock A P and Brion C E 1980 *J. Phys. B: At. Mol. Phys.* **13** 3269-73

Kazansky A and Kabachnik N M *to be published*

LeBrun T, Southworth S H, Armen G B, MacDonald M A and Azuma Y 1999 *Phys. Rev.* A **60** 4667

Levin J C, Biedermann C, Keller N, Liljeby L, O C-S, Short R T, Sellin I A and Lindle D W 1990 *Phys. Rev. Lett.* **65** 988

Lu Y, Stolte W C and Samson J A R 1998 *Phys. Rev.* A **58** 2828

Ohashi H, Ishiguro E, Tamenori Y, Okumura H, Hiraya A, Yoshida H, Senba Y, Okada K, Saito N, Suzuki I H, Ueda K, Ibuki T, Nagaoka S, Koyano I and Ishikawa T 2001 *Nucl. Instrum. Methods A* **467-468** 533

Okada K, Kosugi M, Fujii A, Nagaoka S, Ibuki T, Samori S, Tamenory Y, Ohashi H, Suzuki I H and Ohno K 2005 *J. Phys. B: At. Mol. Opt. Phys.* **38** 421

Pahl E, Meyer H-D and Cederbaum L S 1996 *Z. Phys. D* **38** 215

Persson W 1971 *Physica Scripta* **3** 133

Persson W, Wahlström C-G, Jönsson L and Rocco H O D 1991 *Phys. Rev.* A **43** 4791

Russek A and Mehlhorn W 1986 *J. Phys. B: Atom. Molec. Phys.* **19** 911

Sæthre L J, Thomas T D and Ungier L 1984 *J. Electron Spectrosc. Relat. Phenom.* **33** 381-6
Samson J A R, Stolte W C, He Z X, Cutler J N and Hansen D 1996 *Phys. Rev.* A **54** 2099
Samson J A R, Lu Y and Stolte W C 1997 *Phys. Rev.* A **56** R2530
Schmidt V 1997 *Electron Spectrometry of Atoms using Synchrotron Radiation* (Cambridge:Cambridge University Press) p 152
Sheinerman S A 2003 *J. Phys. B: At. Mol. Opt. Phys.* **36** 4435
Tanaka T, Hara T, Oura M, Ohashi H, Kimura H, Goto S, Suzuki Y and Kitamura H 1999 *Rev. Sci. Instrum.* **70** 4153
Tulkki J, Åberg T, Whitfield S B and Crasemann B 1990 *Phys. Rev.* A **41** 181
Ueda K, West J B, Kabachnik N M, Sato Y, Ross K J, Beyer H J, Hamdy H and Kleinpoppen H 1996 *Phys. Rev.* A **54** 490
Whitfield S B, Tulkki J and Åberg T 1991 *Phys. Rev.* A **44** R6983